



Calculation of The Effects of Fly Ash in Concrete Samples Used as Construction Materials on Radiation Shielding Efficiency Using EGS4 Code

Esra YILMAZ BAYRAK

Gümüşhane University, Torul Vocational School, Department of Medical Services and Techniques, 29800 Torul, Gümüşhane, Türkiye

Received: 05.12.2023

Accepted: 26.01.2024

Published: 19.03.2024

How to cite: Yılmaz Bayrak, E. (2024). Calculation of The Effects of Fly Ash in Concrete Samples Used as Construction Materials on Radiation Shielding Efficiency Using EGS4 Code. *J. Anatolian Env. and Anim. Sciences*, 9(1), 53-59. <https://doi.org/10.35229/jaes.1399774>

Atıf yapmak için: Yılmaz Bayrak, E. (2024). İnşaat Malzemesi Olarak Kullanılan Beton Örneklerinde Uçucu Külün Radyasyon Koruma Etkinliği Üzerindeki Etkilerinin EGS4 Kodu Kullanılarak Hesaplanması. *Anadolu Çev. ve Hay. Dergisi*, 9(1), 53-59. <https://doi.org/10.35229/jaes.1399774>

* <https://orcid.org/0000-0001-5145-0130>

*Corresponding author's:

Esra YILMAZ BAYRAK

Gümüşhane University, Torul Vocational School, Department of Medical Services and Techniques, 29800 Torul, Gümüşhane, Türkiye
✉: esrayilmaz.bayrak@gumushane.edu.tr

Abstract: The aim of this study is to determine the effects of reducing cement and replacing it with fly ash in concrete samples used as construction materials on the radiation shielding efficiency. The radiation shielding effect of concrete samples was determined using the EGS4 code. By contrasting the outcomes with XCOM data, theoretical discussion was conducted. At gamma ray energies between 59.5 and 1332 keV, the mass attenuation coefficients (μ/p) of concrete samples mixed with fly ash were theoretically investigated using WinXCOM and EGS4. Then, several shielding parameters, including mean free path (MFP), half value layer (HVL), radiation protection efficiency (RPE), effective atomic number (Zeff), and gamma-ray kerma coefficients (ky), were found using the mass attenuation coefficients. It has been noted that the parameters governing radiation shielding performance of concrete samples used as building materials are altered when cement is reduced and fly ash is substituted.

Keywords: EGS4 code, fly-ash concrete, mass attenuation coefficient, γ -kerma coefficient.

İnşaat Malzemesi Olarak Kullanılan Beton Örneklerinde Uçucu Külün Radyasyon Koruma Etkinliği Üzerindeki Etkilerinin EGS4 Kodu Kullanılarak Hesaplanması

Öz: Bu çalışmanın temel amacı, inşaat malzemesi olarak kullanılan beton örneklerinde çimentonun azaltılarak ve yerine uçucu kül kullanılmasıyla radyasyon koruma etkinliği üzerindeki etkilerini belirlemektir. Beton örneklerinin radyasyon koruma etkinliği, EGS4 kodu kullanılarak hesaplanmış ve teorik olarak XCOM verileri ile karşılaştırılarak tartışılmıştır. 59.5 ile 1332 keV arasındaki gama ışını enerji aralığında, uçucu kül ile karıştırılmış beton örneklerinin kütle soğurma katsayıları (μ/p), teorik olarak incelenmiştir; bu inceleme WinXcom ve EGS4 simülasyonlarıyla gerçekleştirilmiştir. Hesaplanan kütle soğurma katsayıları kullanılarak ortalama serbest yol (MFP), yarı değer tabakası (HVL), radyasyon koruma etkinliği (RPE), etkin atom numarası (Zeff) ve gama ışını kerma katsayıları (ky) gibi çeşitli koruma parametreleri belirlenmiştir. İnşaat malzemesi olarak kullanıldığında betonun bileşiminde çimentonun azaltılması ve uçucu kül eklenmesinin, radyasyon koruma etkinliği üzerinde etkileyici değişikliklere yol açtığı gözlemlenmiştir.

Anahtar kelimeler: EGS4 kodu, kütle soğurma katsayısı, uçucu kül beton, γ -kerma katsayısı.

INTRODUCTION

We are constantly exposed to radiation in every aspect of our daily lives, both naturally and because of technological developments. Concrete and lead are media frequently used as radiation shielding; However, concrete has several disadvantages such as opacity and weight, while the toxicity and lack of structural integrity of lead-based

radiation shielding systems are the most important disadvantages (Tekin et al., 2021). In order to reduce these disadvantages, it is also possible to reduce radiation permeability by adding different amounts to some building materials. Some construction materials used in our living spaces have a very important place in protection from external radiation. The type, thickness and density of the

material used are the most important factors in the absorption of radiation. The understanding of how various materials interact with different types of radiation is crucial, especially in designing spaces where radiation exposure needs to be minimized, such as hospitals, nuclear facilities, or even in everyday living spaces. Adding some percentages of mineral additives to concrete changes absorption parameters such as linear absorption coefficients, mass absorption coefficients, effective atomic numbers, effective electron densities and absorption cross sections. To calculate the mass attenuation coefficients and photon cross sections for elements, compounds, and combinations over a broad energy range, from 1 keV to 100 GeV, Berger and Hubbell (1999) created the XCOM software Berger and Hubbell, Gerward et al. (2001) created WinXCOM, a modified version of XCOM, to improve the software's usability and accessibility (Gerward et al., 2001).

Fly ash is a material widely utilized in cement and concrete production due to its pozzolanic properties, as evidenced by numerous studies in recent years. When used in appropriate proportions and with proper application, it positively influences various properties of concrete and notably enhances its resistance to chemical effects. The sizes of fly ash particles typically range between 0.5 and 200 μm , comprising glassy particles that are predominantly spherical. Their specific surface areas average around 2800-3800 cm^2/g . The density of fly ash depends on its fineness and mineralogical structure; for fly ash consisting of hollow spherical particles, the absolute density averages at around 2.4 gr/cm^3 . Recent studies have employed various approaches to accelerate the pozzolanic reaction of fly ash, leading to its activation and making it a significant contributing material in construction elements. These advancements have paved the way for more effective utilization of fly ash in the construction sector (Görhan et al., 2009). It has also been stated that it would be beneficial to increase the curing temperature to increase the early strength of fly ash concrete (Poon et al., 1999). Some researchers have conducted research on fly ash in different areas. Kavaz et al. (2022) examined gamma absorption in some resin composites. Eke (2023), determined gamma-ray attenuation characteristics in various chemical fertilizers. Tekin et al. (2021) investigated different types of glasses based on the 46V2O5-46P2O5-(8-x) B2O3 xCuO system in terms of their nuclear radiation shielding properties.

In general, it has been observed that mixing fly ash and silica fume with other concrete components shows better photon attenuation properties due to their higher effective atomic number values (Yılmaz et al., 2011). Some researchers were observed that at 59.5 and 661 keV photon energies, the effective atomic numbers and effective electron densities decrease with the addition of fly ash (Hine, 1952; Yılmaz et al., 2011). Otherwise Yılmaz et al. (2001) are

observed that the values of HTV increase with addition of fly ash.

Monte Carlo simulation is a computing method that models and analyses complicated systems or processes through random sampling. When finding analytical solutions is challenging or impossible, it is especially helpful. Numerous disciplines, including the ones you mentioned nuclear physics, nuclear engineering, medical physics, radiation safety management, and reactor design use Monte Carlo simulation as a valuable tool. Because, considering the limitations of experimental research, the financial consequences of conducting each experiment, and the potential harmful effects of ionizing radiation on living cells and tissues, it would be appropriate to use this method (Kavaz et al., 2022). Mass attenuation coefficients and other factors crucial to comprehending gamma-ray interactions were computed using Monte Carlo methods, which simulate the behavior of gamma rays as they go through materials (Tekin et al., 2017; Kaya et al., 2022). In radiation physics, the quantity of energy deposited in a substance by ionizing radiation is referred to as kinetic energy released in materials (KERMA).

Many studies have recently been conducted with the aim of determining the gamma kerma coefficients for a broad range of composite materials (Baltaş, 2020; Olukotun et al., 2018; Kondo et al., 2008). This kind of research often contributes significantly to fields like nuclear engineering, medical physics (e.g., in radiation therapy or diagnostic imaging), and various industries requiring radiation shielding materials.

Recently, it is envisaged that fly ash will be used more effectively as a building material. Considering that previous studies have shown better photon attenuation properties, it has become necessary to have more information about fly ash. Although the radiation properties of fly ash have been examined in previous studies, its radiation absorption effect has not been examined using the Monte Carlo method.

In this study, the mass attenuation coefficients of fly ash mixed concrete samples were theoretically estimated to range from 59.5 to 1332 keV using Monte Carlo EGS4 and WinXCOM. Specific protection parameters, including MFP, HVL, Zeff, RPE, and gamma kerma coefficients ($k\gamma$), were determined using theoretically calculated values of the XCOM and EGS4 mass attenuation coefficient (MAC).

MATERIAL AND METHOD

Monte Carlo Simulation: The current study used EGS4 (Electron Gamma Showers) Nelson and Hirayama to calculate gamma attenuation parameters and kerma coefficients (Nelson et al., 2018). The HPGe detector response was simulated via EGS4 Monte Carlo simulations.

One needs to use a verified random number generator because MC computations depend on random number generation. The EGS4 code was combined with a RANLUX random number generator since research has shown that this combination results in a longer sequence and a comparatively better distribution (Gasparro et al., 2008). The efficiency of the model operate with EGS4 was split into 10.010 energy bins, each with a width of 0.3 keV.

When the computed area is rotated 360 degrees on the -axis shown in Figure 1, 241 cells are formed, yielding a cylindrical geometry. Assumedly, Figure 1 depicts a sequence of circular projectiles that are cylindrical in shape. The projectiles are identified by their respective planes (P1, P2, ...), and their respective radii (R1, R2, ..., R11). For the point radioactive source, a section of code was written so that all photons were released along the z-axis, producing a collimated photon beam (Baltaş, 2020; Kaya et al., 2022; Celik & Cevik, 2010; Kaya, 2023).

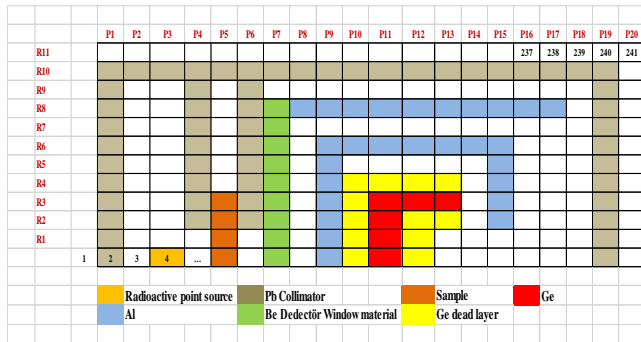


Figure 1. Detector model for Monte Carlo (ESG4 code) calculations.

The MAC parameters that EGS4 uses have an approximate uncertainty of 2%. By performing calculations for gamma photons with energies of 59.5, 122, 383, 662, and 1332 keV, mass absorption coefficients were found. Less than 1% separates the simulated values' relative errors. As a result, we calculated that there was roughly 3% of overall uncertainty.

Gamma attenuation parameters: The mass attenuation coefficients (MAC) parameters of five different concretes mixed with fly ash were found to be as follows in this study:

The Beer-Lambert law, which states the following, can be used to characterize the attenuation of gamma rays in a material:

$$I = I_0 e^{-\mu x} \quad (1)$$

where I is the beam's initial intensity, ε (cm^{-1}) is the material's linear attenuation coefficient for the energy of the gamma rays under consideration, and I is the gamma-ray beam's intensity after it has passed through a thickness of x of the material.

Although the linear attenuation coefficient (μ) is frequently employed to characterize the degree to which a material absorbs gamma rays, it has the disadvantage of

being dependent on the material's density. Consequently, the density-independent mass attenuation coefficient (μ/ρ), which has units of cm^2/g , is frequently more beneficial to use.

$$I = I_0 e^{-(\mu/\rho)\rho x} = I_0 e^{-(\mu/\rho)d} \quad (2)$$

The thickness "d" is expressed in unit area mass of the material (g/cm^2) using the Beer-Lambert law equation. The mass attenuation coefficient (μ/ρ) of a sample that contains multiple metals can be computed using the mixture rule formula, which is as follows:

$$\mu/\rho = \sum_i w_i (\mu/\rho)_i \quad (3)$$

where $(\mu/\rho)_i$ is the density-independent mass attenuation coefficient of the i -th component and w_i is the weight fraction of the i -th component in the sample (Kumar et al., 2020).

A chemical component's weight fraction (w_i) in a mixture can be computed by applying the following relation:

$$w_i = \frac{a_i A_i}{\sum a_i A_i} \quad (4)$$

where a_i is the number of formula units, A_i is the atomic weight of the i -th element, and the summation is taken over all components in the mixture.

where is the formula unit count, The summation of all the components in the mixture is represented by A_i , which is the atomic weight of the i -th element.

In the energy range of 0.0595–1.332 MeV, the mass attenuation coefficients (μ/ρ) of the samples under investigation are calculated using the MC-EGS4 simulation code and compared to the findings of WinXCOM. Using WinXCom software, the samples' theoretical mass attenuation coefficients (μ/ρ) were calculated (Gerward et al., 2001; Baltaş, 2020; Celik & Cevik, 2010; Gerward et al., 2004).

A parameter that is frequently used for determining a material's efficiency in radiation shielding is its effective atomic number, or Z_{eff} . Z_{eff} is a weighted average of a material's constituent atoms' atomic numbers, considering the quantity and energy of incident photons or particles. Because it offers a practical means of comparing the radiation attenuation characteristics of various materials, the Z_{eff} concept is especially helpful in radiation shielding applications. The following formula (Tekin et al., 2019) has been used to calculate the Z_{eff} of the samples that are being studied:

$$Z_{eff} = \frac{\sum f_i A_i (\frac{\mu}{\rho})_i}{\sum \frac{f_i A_i (\frac{\mu}{\rho})_i}{Z_i}} \quad (5)$$

where f_i is weight fraction of the i -th element, A_i is the atomic weight of the i -th element, Z_i is the atomic number of the i -th element in the material (Obaid et al., 2018).

The material's half value layer (HVL) is the thickness that lowers the amount of radiation that goes into it by half (Attix, 2018): The following formula can be used to determine the HVL.

$$HVL = \frac{0.693}{\mu} \tag{6}$$

The average distance a particle or photon may pass through a material before interacting with it in any way (for example, by absorption, scattering, or transmission) is known as the mean free path, or MFP. The MFP is typically calculated as the inverse of a material's linear attenuation coefficient (μ), which expresses the amount of radiation absorbed or scattered per unit length of the material. μ values were used to calculate the mean free path (MFP) in the following manner:

$$MFP = \frac{1}{\mu} \tag{7}$$

where, μ is the linear attenuation coefficient, whose unit of measurement is cm^{-1} . Investigations were conducted on the samples' radiation protection efficiency (RPE) parameter. According to incoming and transmitted photon densities, the efficiency (RPE) is expressed by the following equation (Gaikwad et al., 2019):

$$RPE = \left(1 - \frac{I}{I_0}\right) * 100 \tag{8}$$

Determination of Kerma Coefficient ($k\phi$): Kinetic Energy Released per unit Mass, or Kerma, is a unit of measurement used to quantify the energy transferred from ionizing radiation to the material it passes through. Stated differently, it can be expressed as the product of the initial kinetic energies of all charged particles released by the incident radiation and the material's mass. The energy deposited per unit mass in the target material is measured by the absorbed dose, which considers both the charged particles' initial kinetic energy and their subsequent interactions with the substance.

It is expressed as the total initial kinetic energy, divided by the mass of the material, of all the charged particles (positrons and electrons) freed by incident radiation as it passes through it:

The mass attenuation coefficient and partial interaction probability can be used to compute the Kerma coefficient ($\text{Gy}\cdot\text{cm}^2/\text{photon}$) for uncharged particles. The following equation provides it:

$$K = k\phi \left[\frac{\mu_{tr}}{\rho} \right] \tag{9}$$

where K is uncharged radiation of energy, $k\phi$ is the kerma coefficient and μ_{tr}/ρ is the mass energy-transfer coefficient of the substance (Thomas, 2012):

$$k_{ex}(E) = k_D \sum_i w^i [(\mu_{tr}/\rho)_{\tau,Ex}^i E + \bar{f}_c (\mu_{tr}/\rho)_{c,Ex}^i E + (\mu_{tr}/\rho)_{k,Ex}^i (E - 1.022)] \tag{10}$$

$$k_i(E) = k_D \sum_i w^i [(\mu_{tr}/\rho)_{\tau,i}^i E + \bar{f}_c (\mu_{tr}/\rho)_{c,i}^i E + (\mu_{tr}/\rho)_{k,i}^i (E - 1.022)] \tag{11}$$

Previous works have provided methods for determining the photon kerma coefficients of samples (Baltaş, 2020; El-Khayatt, 2017; Attix, 2008; Abdel-Rahman & Podgorsak, 2010).

RESULTS AND DISCUSSION

Table 1 presents the values of the half value layer (HVL), mean free path (MFP), determined EGS4 and XCOM mass attenuation coefficients μ/ρ ($\text{cm}^2 \text{g}^{-1}$), and samples at different energies: 59.5, 122, 383, 662, and 1332 keV. Table 2 shows the values for the samples' effective atomic number (Z_{eff}), radiation protection efficiency (RPE), theoretical (K_T), and simulated (K_{EGS4}) kerma coefficients. Change graph of HVL and MFP values as an indicator of photon energy for concrete samples containing fly ash Figures 2 and 3, respectively, the energy variation with half value layer (HVL) and mean free path (MFP) for the supplied samples plotted in the 1 keV–100 MeV energy range.

Calculated EGS4 and XCOM mass attenuation coefficients μ/ρ ($\text{cm}^2 \text{g}^{-1}$), values of half value layer (HVL), mean free path (MFP) of samples at different energies 59.5, 122, 383, 662 and 1332 keV have been given in Table 1. The values effective atomic number (Z_{eff}), radiation protection efficiency (RPE) and theoretical (K_T) and simulation (K_{EGS4}) kerma coefficients for the fly ash samples have been given in Table 2. The change in HVL and MFP values of fly ash mixed concrete samples as a function of photon energy is plotted as a function of photon energy. The energy change and mean path for samples with a half value layer (HVL) are plotted in the energy range from 1 keV to 100 MeV and shown in Figures 2 and 3. These graphs show that the half-value layer and mean free path values for the samples increase proportionally with increasing photon energy.

Furthermore, it was observed that the samples under examination had greater HVL and MFP values as the fly ash contribution rose when the values were compared from the figures. More thickness is required to halve the intensity of radiation travelling through a material as its ability to reduce radiation decreases with increasing half value layer (HVL) and mean free path (MFP) values. Consequently, HVL and MFP values rise with photon energy, suggesting that the material gets more transparent to photons with higher energy. Higher photon shielding qualities in samples are correlated with lower HVL and MFP values. Figure 4 displays the variation of Z_{eff} with photon energy in all samples.

Table 1. EGS4 (calculated) and (XCOM) (theoretical) values of mass attenuation coefficients μ/ρ (cm^2/g), HVL and MFP.

	Fly-ash Density (g/cm^3)	Energy									
		Pure 2.148		%5 2.048		%10 2.047		%20 1.977		%30 1.885	
		59.54 keV		122 keV		383 keV		662 keV		1332 keV	
Samples	EGS4	XCOM	EGS4	XCOM	EGS4	XCOM	EGS4	XCOM	EGS4	XCOM	
Mass attenuation coefficients μ/ρ (cm^2/g)	Pure	0.308	0.300	0.157	0.158	0.098	0.097	0.085	0.077	0.064	0.055
	%5	0.294	0.297	0.157	0.158	0.093	0.098	0.073	0.077	0.052	0.055
	%10	0.299	0.296	0.153	0.158	0.087	0.098	0.081	0.077	0.050	0.055
	%20	0.299	0.293	0.159	0.157	0.095	0.097	0.079	0.077	0.061	0.055
	%30	0.286	0.284	0.155	0.156	0.085	0.097	0.072	0.077	0.061	0.055
Half value layer (HVL)	Pure	1.047	1.073	2.054	2.043	3.291	3.312	3.794	4.191	5.039	5.875
	%5	1.150	1.137	2.154	2.144	3.637	3.466	4.633	4.384	6.505	6.146
	%10	1.132	1.143	2.213	2.148	3.891	3.470	4.179	4.388	6.770	6.152
	%20	1.172	1.193	2.204	2.228	3.689	3.593	4.436	4.544	5.745	6.369
	%30	1.229	1.293	2.371	2.354	4.324	3.770	5.104	4.766	6.025	6.681
Mean free path (MFP)	Pure	1.511	1.548	2.964	2.948	4.748	4.779	5.474	6.046	7.270	8.475
	%5	1.660	1.640	3.108	3.094	5.247	5.001	6.685	6.325	9.385	8.867
	%10	1.633	1.649	3.192	3.099	5.614	5.005	6.030	6.331	9.770	8.875
	%20	1.691	1.721	3.180	3.215	5.322	5.183	6.400	6.555	8.288	9.189
	%30	1.773	1.865	3.421	3.396	6.238	5.439	7.364	6.876	8.692	9.638

Table 2. Calculated (EGS4) and Theoretical (XCOM) values of effective atomic number (Z_{eff}) values, Radiation protection efficiency (%) and kerma coefficients k_{γ} (in $\text{pGy}\cdot\text{cm}^2/\text{photon}$)

	Energy Samples	59.54 keV		122 keV		383 keV		662 keV		1332 keV	
		EGS4	XCOM	EGS4	XCOM	EGS4	XCOM	EGS4	XCOM	EGS4	XCOM
Radiation protection efficiency (%)	Pure	60.46	59.50	37.80	37.80	25.74	25.38	20.48	20.66	17.57	15.22
	%5	57.11	57.53	36.43	36.49	23.69	24.48	19.17	19.91	13.98	14.65
	%10	58.05	57.60	35.84	36.64	21.88	24.62	20.97	20.02	11.79	14.73
	%20	61.64	60.88	39.85	39.50	26.23	26.78	22.33	21.84	17.91	16.12
	%30	57.26	56.98	36.99	37.07	21.59	25.11	19.13	20.44	16.64	15.05
Effective atomic number (Z_{eff})	Pure	12.50	12.19	10.67	10.73	10.46	10.39	10.78	10.37	10.96	10.37
	%5	12.01	12.06	10.73	10.78	10.20	10.48	10.04	10.46	10.27	10.46
	%10	12.15	12.03	10.45	10.76	10.19	10.47	10.04	10.45	10.07	10.44
	%20	12.18	11.96	10.84	10.72	10.16	10.44	10.67	10.42	10.99	10.42
	%30	11.78	11.70	10.59	10.58	10.08	10.34	10.05	10.33	10.89	10.32
Kerma coefficients k_{γ} (in $\text{pGy}\cdot\text{cm}^2/\text{photon}$)	Pure	1.268	1.238	0.656	0.660	1.824	1.812	3.433	3.108	6.532	5.599
	%5	1.188	1.203	0.647	0.651	1.730	1.815	2.948	3.115	5.307	5.613
	%10	1.202	1.192	0.630	0.648	1.618	1.815	3.271	3.115	5.103	5.612
	%20	1.191	1.170	0.650	0.643	1.767	1.814	3.190	3.114	6.226	5.611
	%30	1.093	1.087	0.621	0.625	1.580	1.812	2.908	3.113	6.226	5.610

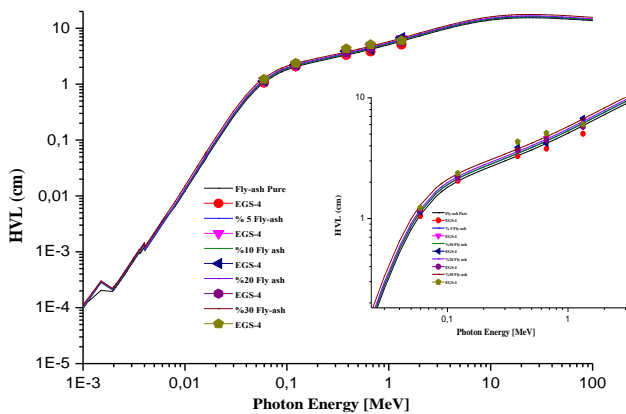


Figure 2. The variation of the half value layer (HVL) with the energy for fly-ash-mixed concrete samples.

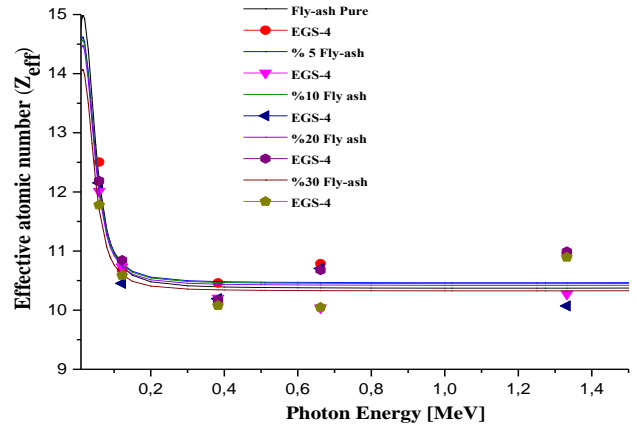


Fig. 4. The variation of effective atomic numbers Z_{eff} of samples versus the photon energy

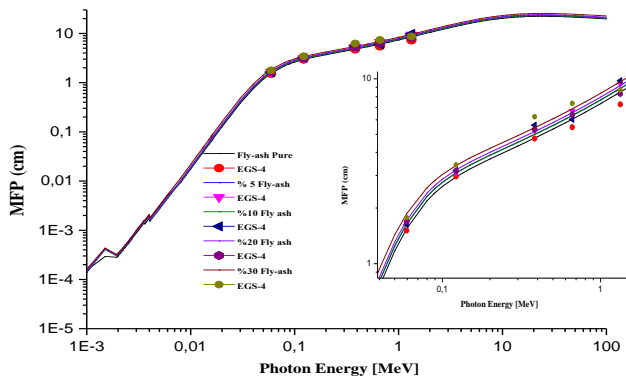


Figure 3. The variation of the mean free path (MFP) with the energy for with the energy for fly-ash-mixed concrete samples.

Fly-ash-mixed concrete samples differ in Z_{eff} values depending on their chemical composition. Figure 5 shows changes of RPE with photon energy for investigated samples. In Figure 5, it is seen that the RPE values decrease as the photon energy increases.

Figure 6 displays the graph of the change in gamma kerma coefficients for the samples. For every energy, the samples' kerma coefficients are the same. The complete energy of incoming photons is transferred to inner-shell electrons in the photoelectric effect, ejecting the electrons from the atom and producing photoelectrons. The material's atomic number has a major influence on this impact. Because higher Z materials have more electrons and corresponding binding energies, the likelihood of this

interaction happening increases as the atomic number increases.

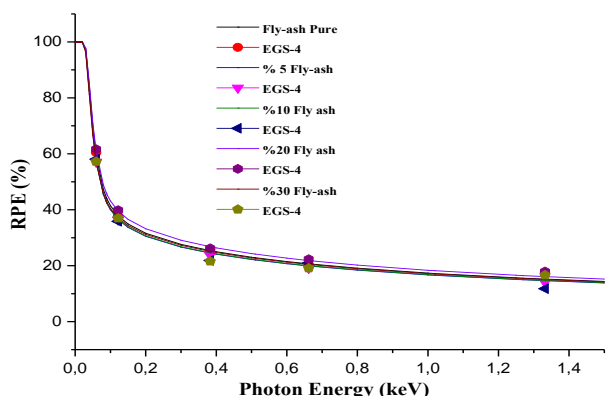


Figure 5. The variation of radiation protection efficiency (RPE) of samples versus the photon energy.

As a result, there is a greater chance that the material will absorb photons through the photoelectric effect. The energy released per unit mass in a material because of ionizing radiation interactions is measured by the Kerma coefficient, which rises as the photoelectric effect becomes more prevalent at lower energies. This is because in materials with higher atomic numbers, the photoelectric effect tends to predominate, resulting in greater energy deposition and higher Kerma coefficients. Thus, increasing atomic number, photoelectric effect prevalence, and the ensuing rise in Kerma coefficients at lower energies are all related and important in understanding the behavior of varied materials when exposed to low-energy gamma radiation.

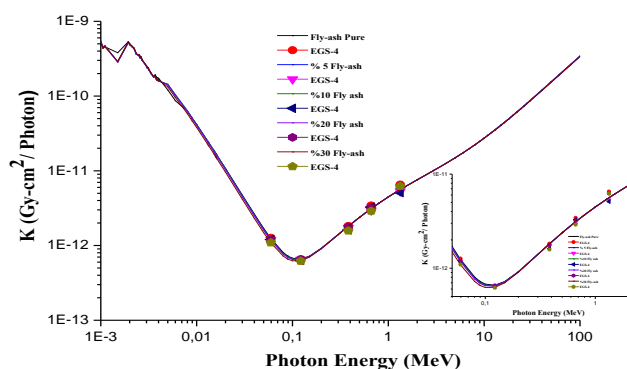


Figure 6. The gamma kerma coefficients of samples as a function of photon energy.

CONCLUSION

Therefore, for gamma energies ranging from 59.5 to 1332 keV, the radiation protection properties of concrete samples mixed with fly ash were examined in this work. Using the EGS4 Monte Carlo simulation package, mass attenuation coefficients (MAC), HVL, MFP, Zeff, RPE, and gamma ray kerma coefficients (k_γ) were assessed for

fly-ash-mixed concrete samples at gamma energies of 59.5, 122, 383, 662, and 1332 keV. The WinXCom program was used to calculate and plot the variation in radiation shielding characteristics for samples in the energy range of 1 keV to 100 MeV. Gamma-ray kerma (k_γ), RPE, MAC (μ/ρ), and Zeff values are all highly dependent on the incident photon energy of the material that the gamma rays pass through.

Up to the first 300 keV, there is a significant drop in the mass attenuation coefficients for concrete samples as the fly ash contribution rises. It was discovered that the half value layer (HVL) and mean free path (MFP) values were higher and the radiation protection efficiency (RPE) for concrete samples decreased as the fly ash contribution rose. The results of this study will be crucial in calculating the level of radiation protection in concrete samples, guaranteeing worker safety, maximum protection intervals, complying with regulatory standards, and starting intervals for the choice of radiation-exposed materials and facility layout.

REFERENCES

- Abdel-Rahman, W. & Podgorsak, E.B. (2010).** Energy transfer and energy absorption in photon interactions with matter revisited: A step-by-step illustrated approach. *Radiation Physics and Chemistry*, **79**(5), 552-566. DOI: [10.1016/j.radphyschem.2010.01.007](https://doi.org/10.1016/j.radphyschem.2010.01.007)
- Attix, F.H. (2008).** *Introduction to Radiological Physics and Radiation Dosimetry*. John Wiley & Sons, U.S.A.
- Baltas, H. (2020).** Evaluation of gamma attenuation parameters and kerma coefficients of YBaCuO and BiPbSrCaCuO superconductors using EGS4 code. *Radiation Physics and Chemistry*, **166**, 108517. DOI: [10.1016/j.radphyschem.2019.108517](https://doi.org/10.1016/j.radphyschem.2019.108517)
- Berger, M.J. & Hubbell, J.H. (1999).** XCOM: Photon cross-sections on a personnel computer (version 1.2). NBSIR85-3597, National Bureau of Standards, Gaithersburg, MD, USA, for version, 3.
- Celik, N. & Cevik, U. (2010).** Monte Carlo determination of water concentration effect on gamma-ray detection efficiency in soil samples. *Appl. Radiat. Isot.* **68**, 1150-1153. DOI: [10.1016/j.apradiso.2010.01.031](https://doi.org/10.1016/j.apradiso.2010.01.031)
- Eke, C. (2023).** Gamma-Ray Attenuation Characteristic of Various Chemical Fertilizers. *Instruments and Experimental Techniques*, **66**(1), 111-118. DOI: [10.1134/S0020441223010098](https://doi.org/10.1134/S0020441223010098)
- El-Khayatt, A.M. & Vega-Carrillo, H.R. (2015).** Photon and neutron kerma coefficients for polymer gel dosimeters. *Nucl. Instruments Methods Phys. Res. Sect. A Accel. Spectrometers, Detect. Assoc. Equip.* **792**, 6-10. DOI: [10.1016/j.nima.2015.04.033](https://doi.org/10.1016/j.nima.2015.04.033)

- El-Khayatt, A.M. (2017).** Semi-empirical determination of gamma-ray kerma coefficients for materials of shielding and dosimetry from mass attenuation coefficients. *Prog. Nucl. Energy*, **98**, 277-284. DOI: [10.1016/j.pnucene.2017.04.006](https://doi.org/10.1016/j.pnucene.2017.04.006)
- Gaikwad, D.K., Sayyed, M.I., Botewad, S.N., Obaid, S.S., Khattari, Z.Y., Gawai, U.P., Afaneh, F., Shirshat, M.D. & Pawar, P.P. (2019).** Physical, structural, optical investigation and shielding features of tungsten bismuth tellurite based glasses. *J. Non. Cryst. Solids*, **503**, 158-168. DOI: [10.1016/j.jnoncrysol.2018.09.038](https://doi.org/10.1016/j.jnoncrysol.2018.09.038)
- Gasparro, J., Hult, M., Johnston, P.N. & Tagziria, H. (2008).** Monte Carlo modelling of germanium crystals that are tilted and have rounded front edges. *Nucl. Instruments Methods Phys. Res. Sect. A Accel. Spectrometers, Detect. Assoc. Equip.* **594**, 196-201. DOI: [10.1016/j.nima.2008.06.022](https://doi.org/10.1016/j.nima.2008.06.022)
- Gerward, L., Guilbert, N., Jensen, K.B. & Leving, H. (2001).** X-ray absorption in matter. Reengineering XCOM. *Radiat. Phys. Chem.* **60**, 23-24. DOI: [10.1016/S0969-806X\(00\)00324-8](https://doi.org/10.1016/S0969-806X(00)00324-8)
- Gerward, L., Guilbert, N., Jensen, K.B. & Leving, H. (2004).** WinXCom-a program for calculating X-ray attenuation coefficients. *Radiat. Phys. Chem.* **71**, 653-654. DOI: [10.1016/j.radphyschem.2004.04.040](https://doi.org/10.1016/j.radphyschem.2004.04.040)
- Görhan, G., Kahraman, E., Başpınar, M.S. & Demir, İ. (2016).** Uçucu Kül Bölüm II: Kimyasal, Mineralojik ve Morfolojik Özellikler. *Yapı Teknolojileri Elektronik Dergisi*, **5**(2), 33-42.
- Hine, G.J. (1952).** The effective atomic numbers of materials for various gamma processes. *Phys. Rev.*, **85**, 725.
- Kaya, S., Çelik, N. & Bayram, T. (2022).** Effect of front, lateral and back dead layer thicknesses of a HPGe detector on full energy peak efficiency. *Nuclear Instruments and Methods in Physics Research Section A: Accelerators, Spectrometers, Detectors and Associated Equipment*, **1029**, 166401. DOI: [10.1016/j.nima.2022.166401](https://doi.org/10.1016/j.nima.2022.166401)
- Kaya, S. (2023).** Calculation of the effects of silver (Ag) dopant on radiation shielding efficiency of BiPbSrCaCuO superconductor ceramics using EGS4 code. *Applied Sciences*, **13**(14), 8358. DOI: [10.3390/app13148358](https://doi.org/10.3390/app13148358)
- Kavaz, E., Tekin, H.O., 2, Zakaly, H.M.H., Issa, S.A.M., Kara, U., Al-Buriah, M.S., Salah, S., Matori, K.M. & Zaid, M.H.M. (2022).** Structural and Gamma-Ray Attenuation Properties of Different Resin Composites for Radiation Shielding Applications. *Brazilian Journal of Physics*, **52**(157), 1-9. DOI: [10.1007/s13538-022-01157-w](https://doi.org/10.1007/s13538-022-01157-w)
- Kondo, K., Ochiai, K., Murata, I. & Konno, C. (2008).** Verification of KERMA factor for beryllium at neutron energy of 14.2 MeV based on charged-particle measurement. *Fusion Engineering and Design*, **83**, 1674-1677. DOI: [10.1016/j.fusengdes.2008.06.008](https://doi.org/10.1016/j.fusengdes.2008.06.008)
- Kumar, A., Gaikwad, D.K., Obaid, S.S., Tekin, H.O., Agar, O. & Sayyed, M.I. (2020).** Experimental studies and Monte Carlo simulations on gamma ray shielding competence of (30+ x) PbO10WO₃ 10Na₂O–10MgO–(40-x) B₂O₃ glasses. *Prog. Nucl. Energy*, **119**, 103047. DOI: [10.1016/j.pnucene.2019.103047](https://doi.org/10.1016/j.pnucene.2019.103047)
- Nelson, W.R., Rogers, D.W.O. & Hirayama, H. (1985).** The EGS4 code system.
- Obaid, S.S., Sayyed, M.I., Gaikwad, D.K. & Pawar, P.P. (2018).** Attenuation coefficients and exposure buildup factor of some rocks for gamma ray shielding applications. *Radiation Physics and Chemistry*, **148**, 86-94. DOI: [10.1016/j.radphyschem.2018.02.026](https://doi.org/10.1016/j.radphyschem.2018.02.026)
- Olukotun, S.F., Gbenu, S.T., Ibitoye, F.I., Oladejo, O.F., Shittu, H.O., Fasasi, M.K. & Balogun, F.A. (2018).** Investigation of gamma radiation shielding capability of two clay materials. *Nucl. Eng. Technol.*, **50**, 957-962. DOI: [10.1016/j.net.2018.05.003](https://doi.org/10.1016/j.net.2018.05.003)
- Poon, C.S., Kou, S.C., Lam, L. & Lin, Z.S. (1999).** An Innovative Method in Producing High Early Strength PFA Concrete. *Modern Concrete Materials; Binders, Additives and Admixtures*, 131-138, ISBN: 0727728229, Thomas Telford Pres.
- Tekin, H.O., Singh, V.P. & Manici, T. (2017).** Effects of micro-sized and nano-sized WO₃ on mass attenuation coefficients of concrete by using MCNPX code. *Appl. Radiat. Isot.*, **121**, 122-125. DOI: [10.1016/j.apradiso.2016.12.040](https://doi.org/10.1016/j.apradiso.2016.12.040)
- Tekin, H.O., Altunsoy, E.E., Kavaz, E., Sayyed, M.I., Agar, O. & Kamislioglu, M. (2019).** Photon and neutron shielding performance of boron phosphate glasses for diagnostic radiology facilities. *Results Phys.*, **12**, 1457-1464. DOI: [10.1016/j.rinp.2019.01.060](https://doi.org/10.1016/j.rinp.2019.01.060)
- Tekin, H.O., Bilal, G., Zakaly, H. M. H., Kilic, G., Issa, S. A. M., Ahmed, E. M., Rammah, Y. S. & Ene, A. (2021).** Newly Developed Vanadium-Based Glasses and Their Potential for Nuclear Radiation Shielding Aims: A Monte Carlo Study on Gamma Ray Attenuation Parameters. *Materials*, **14**(3897), 2-19. DOI: [10.3390/ma14143897](https://doi.org/10.3390/ma14143897)
- Thomas, D.J. (2012).** ICRU report 85: Fundamental quantities and units for ionizing radiation.
- Turner, J.E. (2008).** *Atoms, radiation, and radiation protection*. John Wiley & Sons.
- Yilmaz, E., Baltas, H., Kiris, E., Ustabas, I., Cevik, U., El-Khayatt, A.M. (2011).** Gamma ray and neutron shielding properties of some concrete materials. *Ann. Nucl. Energy*, **38**, 2204-2212. DOI: [10.1016/j.anucene.2011.06.011](https://doi.org/10.1016/j.anucene.2011.06.011)